Annals of Botany **108**: 1307–1322, 2011
doi:10.1093/aob/mcr244, available online at www.aob.oxfordjournals.org

ANNALS OF BOTANY
Founded 1887

Development and persistence of sandsheaths of *Lyginia barbata* (Restionaceae): relation to root structural development and longevity

Michael W. Shane[1,*], Margaret E. McCully[2], Martin J. Canny[3], John S. Pate[1] and Hans Lambers[1]

[1]*School of Plant Biology, M084, The University of Western Australia, 35 Stirling Highway, Crawley, WA 6009, Australia,* [2]*Plant Industry, CSIRO, Canberra, ACT 2601, Australia and* [3]*Plant Science Division, Research School of Biology, RN Robertson Building, The Australian National University, Canberra, ACT 0200, Australia*
** For correspondence. E-mail michael.shane@uwa.edu.au*

Received: 13 May 2011 Returned for revision: 12 July 2011 Accepted: 2 August 2011 Published electronically: 3 October 2011

• *Background and Aims* Strongly coherent sandsheaths that envelop perennial roots of many monocotyledonous species of arid environments have been described for over a century. This study, for the first time, details the roles played by the structural development of the subtending roots in the formation and persistence of the sheaths.
• *Methods* The structural development of root tissues associated with persistent sandsheaths was studied in *Lyginia barbata*, native to the Western Australian sand plains. Cryo-scanning electron microscopy CSEM, optical microscopy and specific staining methods were applied to fresh, field material. The role of root hairs was clarified by monitoring sheath development in roots separated from the sand profile by fine mesh.
• *Key Results and Conclusions* The formation of the sheaths depends entirely on the numerous living root hairs which extend into the sand and track closely around individual grains enmeshing, by approx. 12 cm from the root tip, a volume of sand more than 14 times that of the subtending root. The longevity of the perennial sheaths depends on the subsequent development of the root hairs and of the epidermis and cortex. Before dying, the root hairs develop cellulosic walls approx. 3 μm thick, incrusted with ferulic acid and lignin, which persist for the life of the sheath. The dead hairs remain in place fused to a persistent platform of sclerified epidermis and outer cortex. The mature cortex comprises this platform, a wide, sclerified inner rim and a lysigenous central region – all dead tissue. We propose that the sandsheath/root hair/epidermis/cortex complex is a structural unit facilitating water and nutrient uptake while the tissues are alive, recycling scarce phosphorus during senescence, and forming, when dead, a persistent essential structure for maintenance of a functional stele in the perennial *Lyginia* roots.

Key words: CSEM, lignified and suberized root hairs, *Lyginia barbata*, perennial drought-tolerant roots, persistent root hairs, phosphorus recycling, Restionaceae, rhizosheaths, root hair histochemistry, sandbinding roots.

INTRODUCTION

The capacity of axile perennial roots for developing persistent sandsheaths is widely expressed across the Restionaceae (Southern Rushes) and desert grasses (Price, 1911; Arber, 1934; Meney and Pate, 1999). The superficial morphology of these sheaths in the rush *Lyginia barbata* was briefly described by Dodd *et al.* (1984), and more recently in studies of seasonal root growth and water status (Shane *et al.*, 2009, 2010). In brief, perennial roots of *L. barbata* are covered by a thick sheath of sand grains trapped tightly by long, tangled, persistent root hairs. This sandsheath effectively doubles the diameter of the root. Sandsheaths of *Lyginia* and other perennial monocotyledons growing in desert and sand dune habitats have been implicated in protection against desiccation and heat stress, especially during summer (Price, 1911; Dodd *et al.*, 1984; Shane *et al.*, 2010).

Shane *et al.* (2009, 2010) measured growth rates and depths of penetration of sandbinding roots in the top 1·5 m of the sand profile. They also reported, for the first time, that young roots of each perennial root system which had not descended beyond this depth before the adjacent sand completely dried out in summer became dormant, resuming growth with the onset of winter rains. Sandsheaths reach the tips of these dormant roots, often completely encasing them, whereas winter-elongating roots are bare for up to 15 mm from their apices (Shane *et al.*, 2009). Sandbinding roots are widespread in desert and sand dune perennial grasses (Wullstein and Pratt, 1981; Buckley, 1982; Danin, 1996; Bailey and Scholes, 1997; Othman *et al.*, 2004) and have been described for well over a century (see Price, 1911; Arber, 1934) but surprisingly little is known of how root development relates to sandsheath formation.

Here we investigate how the structural development and longevity of the sandsheaths of the *Lyginia* axile roots relate to developmental changes in structure and wall histochemistry of the subtending roots. We discuss how these developmental changes may contribute to the functioning of the sheaths. We investigate whether direct contact with root hairs is essential for sandsheath development and stability, or if, as found by Watt *et al.* (1993) in a model system, soil particles cohere strongly to each other in the presence of exudates released from maize roots and rhizosphere bacteria in the absence of root hairs. The magnitude of phosphorus release during cortical senescence is also dicsussed.

MATERIALS AND METHODS

Field sites

Large populations of *Lyginia barbata* R.Br. (Restionaceae, Southern Rushes) were studied on south-western Australian sandplains in undisturbed *Banksia* woodland and associated heathland (2006–2010) at Melaleuca Park (50 km north of Perth, 31°41′S, 115°54′E) and Yule Brook Reserve (25 km south-east of Perth, 32°01′S, 115°58′W). These plants were growing on deep and severely nutrient-impoverished sands of the Bassendean Dune System (McArthur, 1991). The climate of the region is severe Mediterranean with cool, wet winters (June–September) and hot, dry summers (November–February). For additional site information see Shane *et al.* (2009, 2010).

Collection of undisturbed roots in the field

Fresh. More than 100 sheathed axile roots as in Fig. 1 were recovered intact by careful excavation around the base of at least 50 plants between May and September 2006–2010. Current season shallow roots originating near tips of elongating rhizomes, and roots formed earlier (≥ 3 years) on older regions of the rhizomes were collected from the top 0·5 m of sand (for a diagram of roots used see Shane *et al.*, 2010, fig. 1). Roots were wrapped in damp paper towels, sealed in plastic bags and transported to the laboratory in a cool box at approx. 4 °C. These roots were used for measurements of sheaths, root hair density counts and histochemistry.

The tips of a few dormant roots collected in the dry season were also examined.

Cryo-fixed. Whole axile root lengths up to 20 cm or more from tips collected fresh as above were excised and immediately plunged into liquid nitrogen (LN_2) in the field. Frozen pieces (approx. 1 cm) were cut from the desired regions under LN_2, placed in cryo-vials and stored in LN_2 until shipped in a cryo-shipper to the Centre for Advanced Microscopy, Australian National University, Canberra, for cryo-scanning electron microscopy (CSEM).

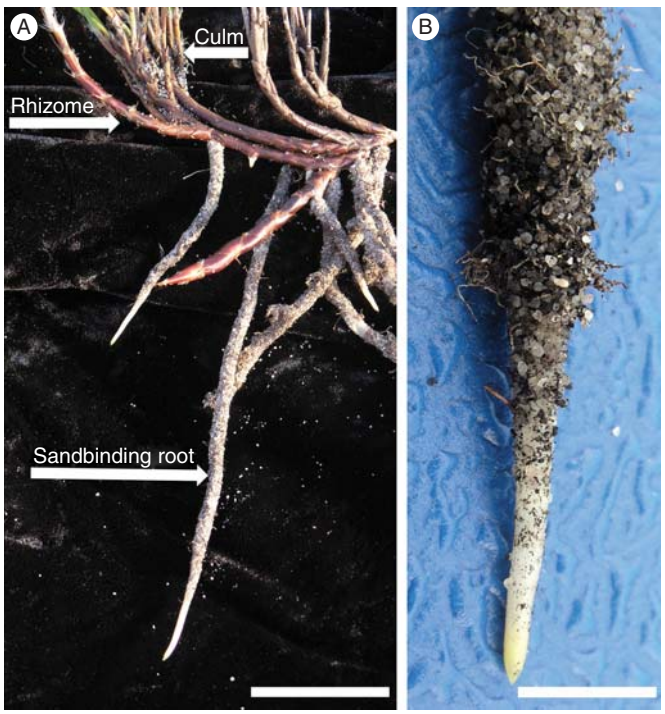

FIG. 1. (A) Root, rhizome and shoot (culm) system of a rush plant excavated during the wet (winter) season. Culms can photosynthesize year-round (Shane *et al.*, 2009). Tough brown scale leaves cover rhizomes which are typically 100–250 mm deep in the sand. Most roots from this study were young, current-season, growing, sandbinding roots located in the upper 0·5 m of topsoil. These roots were initiated near tips of elongating rhizomes and, except for growing tips, were encased in a sandsheath along their entire length. (B) Detail of a growing root tip free of sandsheath. Scale bars: (A) = 50 mm; (B) = 8 mm.

CSEM

Cryo-fixed material. The previously frozen root segments (5–10 mm long) with sandsheaths intact were quickly secured in the groove of a brass holder with carbon paste, plunged into LN_2 and then transferred with a cryo-transfer system (CT 1500; Oxford Instruments, Oxford, UK), to the cold stage of a scanning electron microscope (S360; Cambridge Instruments, Cambridge, UK). Any frost on the surface was sublimed in the microscope column by warming the sample stage to −90 °C while the specimen was continuously observed at 1 kV. The sample was then cooled to −160 °C, coated with evaporated gold and examined at 15 kV. Images from 4–10 replicate root segments were captured digitally.

Maturation and progressive senescence of cortical cells were observed in segments of similar roots whose sandsheaths had been scraped off while still frozen in LN_2. Short segments (approx. 4 mm) were cut under LN_2 at 15, 75 or 180 mm from the tips. Segments were quickly secured to aluminium stubs with Tissue Tek (Torrance, CA, USA) and immediately plunged into LN_2. Segments were planed to a smooth transverse or longitudinal face with a glass knife (followed by a diamond knife) at −90 °C in a cryo-ultramicrotome (FC4; Reichert-Jung, Vienna, Austria). Samples were then transferred with a cryo-transfer system (CT 1500; Oxford Instruments) to the cold stage of a scanning electron microscope (Hitachi 4300 Schottky Field Emission, Tokyo, Japan), etched at −90 °C to reveal cell outlines, cooled to −160 °C and coated with evaporated aluminium. Details of these procedures are given in Huang *et al.* (1994) and McCully *et al.* (2000, 2010). Images from 7–10 replicate roots at 15, 75 and 180 mm from growing apices were captured digitally

Fresh. Some field-collected roots were shipped overnight at ambient temperature to Canberra. These roots were cryo-fixed and examined within 24 h from collection. They were cut into 3- to 4-mm transverse or longitudinal segments with a razor blade from desired regions, affixed to the surface of brass stubs with carbon paste and allowed to dry in air until any water present on tissue surfaces evaporated (2–5 min). Samples were then frozen directly in the preparation chamber of the S360 cryo-scanning electron microscope (Craig and Beaton, 1996), etched and coated with gold. Images of surface morphology from 4–6 replicate roots at 15, 75 and 180 mm from their apices were captured digitally.

Measurements of sandsheaths and underlying root tissues

Sandsheath thickness, volume and root diameters were measured at 20-mm intervals along the region 10–180 mm from the root tips. Transverse sections were cut from fresh roots with a razor blade (sandsheaths typically remained attached). Diameters of the roots (not including the root hairs), and the roots with attached sheaths were measured on the sections (from ten roots from different plants) using digital vernier calipers (Sontax, Zhejiang, China) under a dissecting microscope. Ratios of sheath volume/root volume were determined from these measurements as in Watt *et al.* (1994).

Measurements of root hair density, diameter and wall thickness

Two techniques were used to observe root-hair development and quantify their density in young and mature regions of frozen and fresh samples.

(1) Density was determined directly from CSEM digital images (like Fig. 2) of young regions 2–5 mm from the tip (five roots from five plants). All the root hairs that had emerged within 2–3 replicate areas of 100 – 500 μm^2 were counted on each of the 25 roots and the total numbers calculated for 1 mm^2. To estimate the number of hairs per 1-mm length of root axis, root surface area was multiplied by the number of root hairs per mm^2.
(2) Mean epidermal cell length (in longitudinal sections) and width (in transverse sections) were measured in both young regions 2–5 mm and mature regions 50–100 mm from the root tips. Epidermal cell dimensions were recorded from digital CSEM images, or by optical microscopy of fresh sections using a stage micrometer. Root-hair density was then estimated from those data by calculating the number of epidermal cells across an average surface area of 1 mm^2 of root axis, and by assuming each epidermal cell produced a root hair (as apparent in Fig. 2).

Root hair diameters were measured from digital CSEM images, and wall thickness was determined from transversely fractured hairs which were occasionally included in the CSEM preparations.

Histochemical methods

Hand-cut sections of fresh roots from which most of the sand had been scraped off were stained by the following methods to determine histochemical properties of the cell walls of the root hairs, epidermis and the underlying regions of the cortex along the developing sheathed roots.

(1) Toluidine blue, 0·05 % (w/v) (pH 4·4). Pink to red staining indicates acidic polysaccharides, blue to green, compounds with phenolic components (O'Brien and McCully, 1981).
(2) Rhodamine B (1 : 10 000 aqueous). Fluorescence observed with blue light excitation. Lipid-rich compounds fluoresce yellow to orange (Boerner, 1952).
(3) Phloroglucinol/HCl (Wiesner reaction) (Jensen, 1962). Pink to red colour specific for hydroxycinnamyl aldehyde structures in lignin (Pomar *et al.*, 2002).
(4) Periodic acid-Schiff's (PAS) reaction with appropriate controls (i.e. Schiff's reagent alone) (Jensen, 1962). Polysaccharides with vicinal hydroxyl groups stain red (cellulose often an exception, O'Brien and McCully, 1981).
(5) Schiff's reagent. The aldehyde groups of lignin (and any other endogenous aldehyde groups) will stain red (Jensen, 1962).
(6) Distinction of lignin from ferulic acid. Comparison of UV-induced autofluorescence in water with that in 0·1 M ammonium hydroxide. A shift from blue autofluorescence to green/blue at the high pH indicates ferulic acid (Harris and Hartley, 1976).
(7) Saturated Sudan III and Sudan IV in 70 % EtOH (Pearse, 1968). Suberin and cutin 'stain' red.

Bright-field, epifluorescence and polarizing optics were used with a Zeiss Axiophot (Oberkochen, Germany). Exciter filter BP 450–490, barrier LP 520 was used for rhodamine-induced fluorescence, and exciter G 365, barrier LP 420 for autofluorescence.

Photomicrographs were recorded digitally on a Nikon D700 camera fitted with an eyepiece attachment (Martin Microscope, Easley, SC, USA) and processed using Photoshop CS5 software (San Jose, CA, USA).

Sandsheath formation by roots separated from the soil matrix by mesh

Root mesh frames (300 × 80 mm) were constructed from nylon mesh of 38- or 1-μm pore size (approx. 25 μm thick, Nitex; Sefar, Huntingwood, NSW, Australia) or from polycarbonate membrane of 0·03 μm pore size (approx. 10 μm thick; GE Water and Process Technologies, Trevose, PA, USA). Each long edge of a rectangle of mesh was fastened to a bamboo stick (diameter 4 mm) and the mesh held taut by inserting sticks of the appropriate length into the holes of plastic spacers at both ends to form a frame. In September (2009) roots 10–30 mm long, recently emerged from close to rhizome tips (Fig. 1; see also Shane *et al.*, 2010, fig. 1), were carefully exposed along faces of shallow trenches dug next to the plants. To prevent drying, water was misted onto exposed root surfaces using a spray bottle as necessary. A mesh frame (five frames for each pore size, $n = 15$ roots) was then quickly aligned against the soil matrix with an angle of inclination 50–60° directly below each young root tip so that the root would subsequently grow down and along the upper surface of the mesh. Soil was carefully back-filled over the root and mesh frame, gently compacted and a small amount of water applied to remoisten the soil profile. Positions of each frame were tagged, and they were carefully harvested 10 weeks later. Each frame was shaken free of loose sand, and checked for sandsheaths on the root, and on the underside of the mesh. Frames were photographed, and allowed to air-dry. Subsequent measurements of sandsheath thickness, and observations by CSEM and optical microscopy and staining were carried out as outlined above.

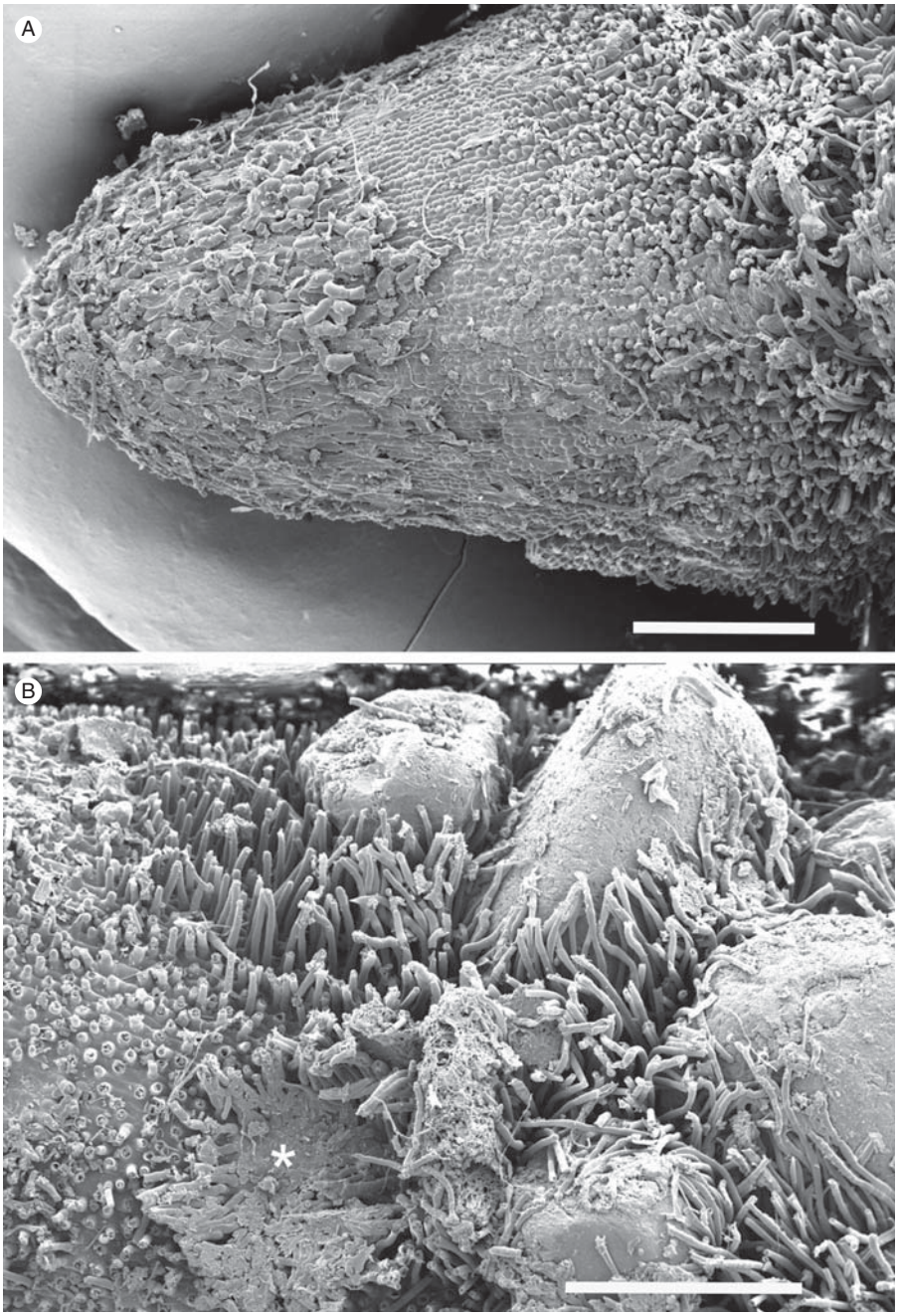

FIG. 2. Young regions of sandbinding roots (as in Fig. 1B) cryo-fixed in the field during the wet (winter) season. Whole mounts (A) approx. 3 mm, (B) 3–5 mm from the tip. (A) The youngest root hairs initiated just beyond the root cap, with no sand attached. Each epidermal cell typically produced a root hair. (B) Further from the tip, the hairs begin to encircle and entrap sand grains and short hairs are exposed between anchored grains. Dense patches of flattened hairs (asterisk) are exposed where sand fell off during sample preparation. CSEM. Scale bars: (A) = 500 μm; (B) = 440 μm.

Phosphorous concentrations along sandbinding roots

Fresh, growing field roots ($n = 7$ from seven plants) were scraped free of sheath. Four segments (0–10, 15–70, 75–130 and 135–200 mm from the tips) were separated, those from each region pooled and dried to constant weight at 70 °C. Segments were ground to a fine powder in a ball mill and digested in concentrated $HNO_3/HCLO_4$ (3 : 1). Total [P] was determined using the Malachite green colorimetric method (Motomizu *et al.*, 1983).

RESULTS

General features of L. barbata

Rhizomes excavated in the field during winter have aerial culms. Perennial sandbinding roots emerge mostly in the vicinity of culms, but also from intercalary regions of the rhizome (Fig. 1A). These roots descend relatively straight and deeply into the sandy substrate. Except for their most distal regions, they are surrounded by a firmly attached sandsheath

(Fig. 1B). Sandsheaths begin to form, on average, 10 ± 2 mm from the bare white tips, but the length of these bare regions is reduced in slower-growing roots harvested during earlier and later parts of the growing season. The bare, clean portions of the root surface (Fig. 1B) more or less coincide with the region of root elongation. Axile roots produced in earlier seasons can persist for several years.

Structure of the surface of the developing sandbinding roots

CSEM of roots cryo-fixed in the field confirmed that tips had normal root caps and a bare soil-free region overlying meristematic and elongation zones (Fig. 2A). Here, cells of the epidermis were in files along the roots and clearly showed that a root hair protruded from every cell (Fig. 2). A few sand grains clung to the extreme tip regions (Fig. 1B), but on surfaces less than 10 mm proximal to tips, early development of sand binding was seen in associations of young root hairs elongating between and around a few sand grains of varying size (Fig. 2B).

As root hairs elongate, they recruit an increasing depth of sand particles into the sheath, increasing its thickness up to six-fold between 10 and 100 mm from the root tip. Over the same distance the ratio of sheath volume to that of the subtending root increased 14-fold (Table 1). Tight enmeshment of the sand was ensured, not only by the extremely high density of hairs (approx. 5900 mm^{-1} root length, Table 2a), but also by their apparent thigmotropic response by which they track and tightly wrap around many of the grains (Fig. 3A, B). At 5 mm from the tip the root hairs were alive, with walls approx. 0·5 μm thick (Fig. 3C) but by 100 mm from the tip the walls were over 3 μm thick and the hairs were dead (Fig. 3D). The dead hairs persist and retain their smooth cylindrical shape even in very old sheaths which persist on the perennial roots (Fig. 4). The strength and rigidity prevent easy removal of the sheath by 100 mm from the root tip where most of the sand could be removed only by scraping. In contrast, it was easy to remove the sheath from younger regions, 20–30 mm from the tip by a vigorous water wash.

Dormant roots had sandsheaths enmeshed by thick-walled root hairs close to (Fig. 3E) or completely covering the root tip (Shane *et al.*, 2009).

TABLE 1. *Measurements of* Lyginia barbata *roots and their surrounding sandsheaths formed at increasing distance from the root apex*

Distance from root apex (mm)	Volume sheath/ volume root	Diameter of root (mm)	Thickness of sheath (mm)
10	0·4 (0·1)	2·0 (0·1)	0·2 (0·06)
20	3·0 (0·5)	1·9 (0·1)	0·7 (0·11)
40	3·0 (0·4)	2·0 (0·1)	1·0 (0·06)
60	3·6 (0·6)	1·9 (0·1)	1·1 (0·07)
80	3·8 (0·6)	2·0 (0·1)	1·2 (0·05)
100	5·9 (0·7)	1·8 (0·1)	1·3 (0·04)
120	5·6 (1·6)	1·9 (0·2)	1·5 (0·17)
140	5·5 (1·6)	1·8 (0·1)	1·4 (0·20)
160	5·1 (1·4)	1·9 (0·1)	1·4 (0·17)
180	4·1 (0·6)	1·9 (0·1)	1·2 (0·07)

Data are means (s.e.), $n = 20$ roots from ten plants.

Structural changes in associated epidermis and cortex during sandsheath development

The distance from the root tip at which the sequence of developmental changes occurs varied with the growth rate of individual roots, and in dormant roots was very short (Fig. 3E; cf. Shane *et al.*, 2010). Figure 5 illustrates a typical developmental sequence of peripheral tissues with accompanying sandsheath development in growing roots. The youngest epidermal cells in the soil-free region close to the root tip are columnar, with a thick outer tangential wall (Fig. 5A), which forms a protective pellicle as in grasses (McCully and Canny, 1994). Other walls of these cells and those of the young cortex are thin, and all cells are intact and closely packed, with only a few small intercellular spaces in the central cortex (Fig. 5B).

At increasing distance from the tip, cells in the central cortex progressively die and are crushed, eventually forming an aerenchymous middle cortex (Figs 5C–G and 3E). This aerenchyma was colonized frequently by actinobacteria (inset, Fig. 5G). Epidermal cells elongated to a more tabular shape, but remained relatively short, each cell retaining a

TABLE 2(a). *Measurements of epidermal cell length and width in roots of* Lyginia barbata

	Root epidermal cell measurements*			Root hair density*			
				Estimated from epidermal cell measurements†,‡		Counted directly§	
Mean root diameter (mm)	Distance from root tip (mm)	Cell length (μm)	Cell width (μm)	No. mm^{-2} root surface	No. mm^{-1} root length	No. mm^{-2} root surface	No. mm^{-1} root length
1·5	2–5	36·8 (2·4)	18·5 (1)	1469	6918	1255 (61)	5898 (450)
2·0	~50	67·9 (2·5)	22·1 (0·8)	666	4185	ND	ND

Values are means (s.e.) of $n = 5$ cells from each of six roots. ND, not determined.
* Measurements made on fresh and cryo-fixed field-grown roots.
† Method 1 (see text).
‡ Assumed that each cell develops a root hair.
§ Method 2 (see text).

TABLE 2(b). *Root hair numbers in mesophytic grasses**

Species	No. mm $^{-1}$ root length	Approx. no. mm $^{-2}$ root surface	Reference
Lolium perenne	88	ND	Reid (1981)
L. perenne	30	40	Robinson and Rorosin (1987)
L. perenne	45	108	Föhse *et al.* (1991)
L. multiflorum	98	142	Drew and Nye (1969)
L. rigidum	300	ND	Hill *et al.* (2010)
L. rigidum	50	62	Schweiger *et al.* (1995)
Festuca rubra	30	67	Boot and Mensink (1990)
Triticum aestivum	46	95	Föhse *et al.* (1991)
Zea mays	161	ND	Reid (1981)
Microlaena stipoides†	900	1150	Hill *et al.*, (2010)
Eragrostis pallens	10, 4·5‡	ND	Bailey and Scholes (1997)
Zea mays§	22	50	Moreno-Espindola *et al.* (2007)
Cynodon dactylon§	24	30	Moreno-Espindola *et al.* (2007)
Saccharum sp.§	140–870¶	ND	Evans (1938)
Poa pratensis§	480	318	Dittmer (1958)
Secale cerale§	570	318	Dittmer (1958)

ND, not determined.

* Where only root hair numbers per mm^{-1} root length, or per mm^{-2} were given, the other density has been calculated here if root diameter measurements were available.

† Australian native perennial.

‡ High number in 80 % sand, low number in 30 % sand.

§ Only these plants were field-grown, all others were seedlings or young plants grown in pots.

¶ Comparable numbers from two different cultivars.

root hair (Fig. 5C). Further from the root tip, cells of both the outer and the inner cortex develop into thick-walled fibres. Epidermal cells, in parallel with their root hairs, also develop thick walls which eventually appear completely coherent with the underlying outer cortical fibres (Fig. 5E–G), forming a strong supporting base which retains the root hairs (and their enmeshed sandsheath) in place. The inner cortical fibres also form a tightly packed inner rim of sclerenchyma (Fig. 5E–G). The endodermis remains distinct from this rim and is easily separated from it during specimen handling (Fig. 5F). The inner and outer rims are held together by remnants of the middle cortical walls (Fig. 5F). With root maturity, both the inner and the outer sclerotized rims become brown (Fig. 4A).

In dormant roots, all these developmental processes at the root surface and within the cortex have proceeded right to the apex (Fig. 3E).

Wall histochemistry of root hairs, epidermal and cortical tissues associated with sandsheath formation

The histochemical reactions on fresh hand-cut sections are illustrated in Fig. 6 and are summarized in Table 3.

With Toluidine blue (Fig. 6A–C), pink to purple metachromasy colours were characteristic of the walls of root hairs and young epidermal cells in the soil-free region close to the root tip (Fig. 6A), indicating acidic polysaccharides. The cortical walls were blue, indicating aromatic compounds. The metachromasy disappeared by 20–30 mm from the tip, replaced by blue in the hair and epidermal walls, indicating masking of the acidic polysaccharide staining by aromatic residues. The cortex walls were strongly blue. The positive test for ferulic acid (Fig. 6J, K) on sections 20 mm from the root tip indicates that the Toluidine blue wall staining was, at least in part, due to ferulic acid incrusted in the walls. The epidermal walls included some dark-brown patches of endogenous pigment (Fig. 6B). At approx. 120 mm from the tip, the central cortex and root hair walls were more greenish blue, and dark-brown endogenous pigment masked and/or prevented any staining of walls of epidermis and narrow regions of both outer and inner cortex (Fig. 6C).

Rhodamine B-induced, yellow to orange fluorescence indicated that the walls of root hairs and epidermis included a lipid-rich component (probably suberin) as close to the root tip as approx. 10 mm (Fig. 6D) and this staining intensified by approx. 20 mm (Fig. 6E). Further from the tip, autofluorescence of aromatic compounds begins to obscure the orange fluorescence, with the result that its origin from a thin outer layer of the root hair walls becomes increasingly clear (Fig. 6F, G, and lower inset G). In other root tissues the underlying autofluorescence obscures any reaction with the fluorochrome (Fig. 6D–F). Endogenous pigment obscures cortical fluorescence by approx. 180 mm from the tip, but the endodermis is still strongly fluorescent (Fig. 6G).

Pale pink to red staining by Phloroglucol/HCl (Fig. 6H, I) indicated progressive lignification of root hairs, epidermis, and inner and outer cortex. Mid-cortical cells remain unlignified. Where present, the endogenous pigment was very dark red to black.

The thick walls of old root hairs were strongly birefringent, and Sudan staining revealed a thin lipid-rich outer layer (upper inset, Fig. 6G).

Sheath formation on root mesh

Of the 15 root mesh frames installed in the field (Fig. 7), ten were colonized by a sandbinding root along its entire length.

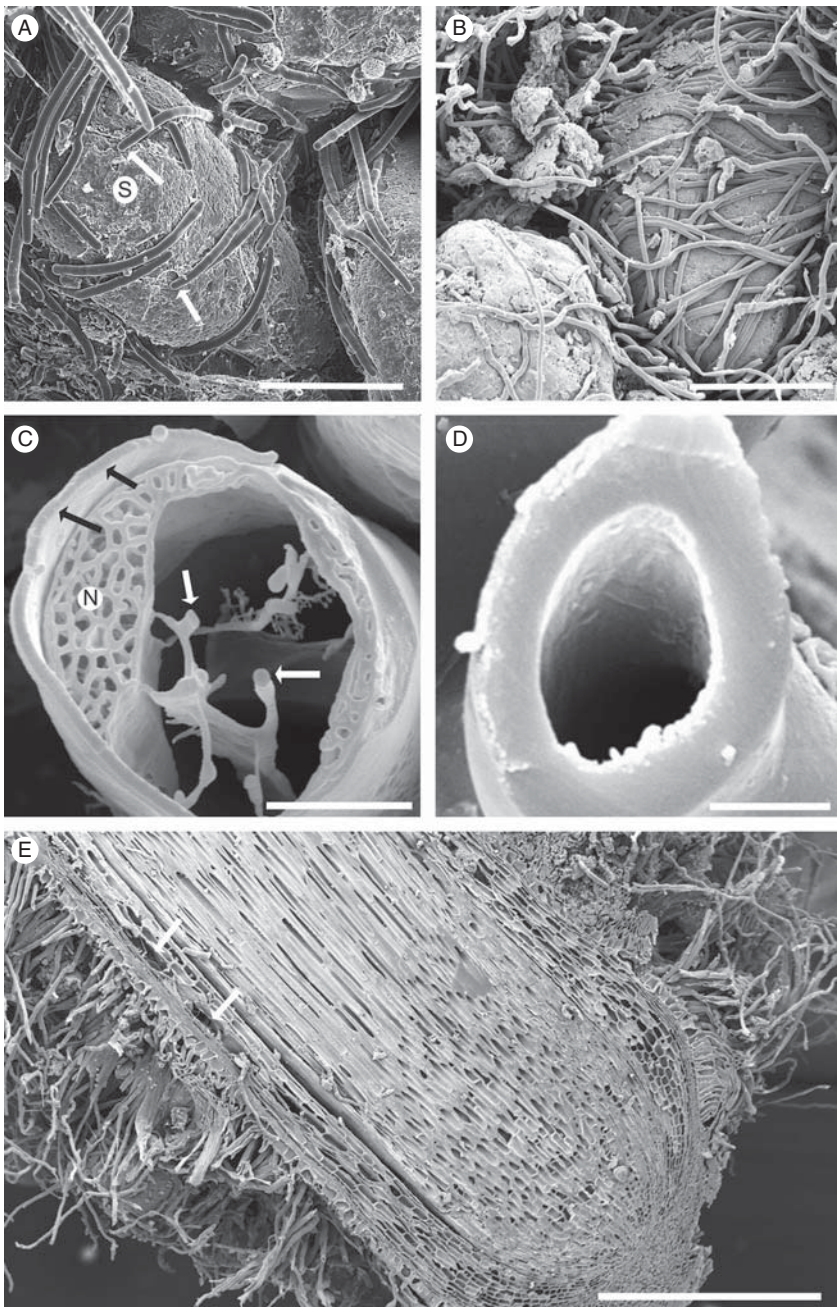

FIG. 3. (A, B) Root hairs enmeshing sand grains (S) at the periphery of developing sandsheaths, approx. 10 and 75 mm, respectively, from the tip of a growing root like that in Fig. 1B. (C, D) Fractured root hairs, at approx. 5 and 100 mm, respectively, from a growing tip. The younger hair was living, with prominent nucleus (N), peripheral and transvacuolar cytoplasm (white arrows), and a relatively thin wall (black arrows). The older hair had developed a very thick wall before death. (E) Longitudinal face of dormant root showing aerenchyma formation in mid-cortex (arrows), and root hairs developed almost to the root tip. CSEM images. Scale bars: (A) = 165 μm; (B) = 375 μm; (C) = 5 μm; (D) = 5·5 μm; (E) = 1·2 mm.

These ten root meshes included at least three from each mesh treatment. In some cases roots failed to grow, probably due to disturbance and/or drying out during installation. Roots that descended down against the upper surface of inclined meshes of 38- or 1-μm pore size constructed sandsheaths on their upper and on the lower surface of the mesh (Fig. 8A–D). Staining of sandsheaths on lower surfaces (Fig. 8C) showed that the root hairs had grown through the mesh and encircled and entrapped sand grains essentially as observed in sandsheaths formed in direct contact with roots elsewhere in the field. Sandsheaths formed on the lower surfaces of 1-μm pore size mesh overlaid by mature root regions were thinner (0·8 ± 0·2 mm, Fig. 8D) compared with those developed below 38-μm pore size mesh (1·3 ± 0·2 mm) which were similar to those measured on untreated roots (Table 1).

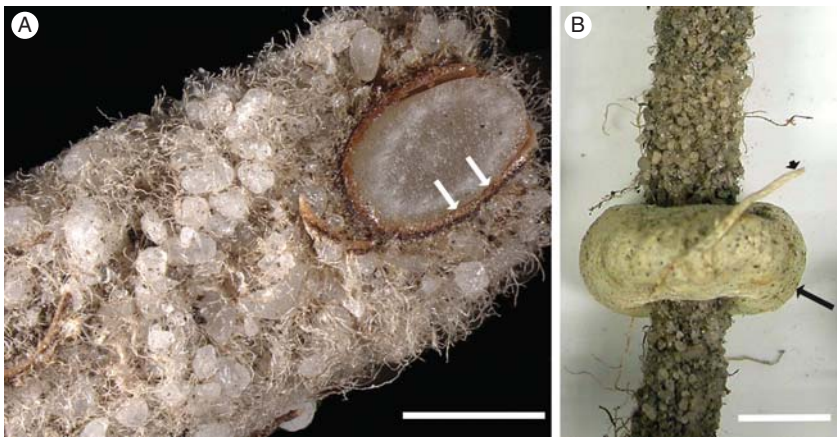

FIG. 4. (A) An oblique cut with a razor blade of a fresh approx. 3-year-old, perennial root with intact, sandsheath and persistent root hairs. Brown collapsed cortex and epidermis (arrows). (B) Sandsheath surrounded by a haustorium (arrow) of the root hemiparasite *Nuytsia floribunda*. A fine *Nuytsia* root (arrowhead) connects haustorium to the parasite. Scale bars: (A) = 1·7 mm; (B) = 4 mm.

Root hair diameter ranged from 8 to 12 μm and they easily penetrated mesh of pore size 38 μm. However fewer, but still a surprising number, managed to grow through 1-μm pore mesh (Fig. 8D) by displacing the nylon fibres (Fig. 8E).

The more rigid polycarbonate membranes (0·03-μm pores) were not penetrated by root hairs, and there was no sand binding on the lower surface. Staining of the polycarbonate mesh with Toluidine blue, by the PAS procedure or by Schiff's reagent alone after removal of the roots revealed that where a root had been in contact with the mesh, there were clear, unstained root hair 'ghosts' (Fig. 9A, B). Mesh between the ghosts stained blue/green with Toluidine blue, and light or strong pink with Schiff's reagent or the PAS reaction, respectively. These staining reactions indicated sparse production of polysaccharide and phenolic exudates by either the root and/or associated microbes, in contrast to the prolific accumulation of mucilage on a nylon membrane traversed by a maize root (Watt *et al.*, 1993; McCully, 1999, fig. 2d).

Mesh beyond the contact region did not stain. The unstained root hair 'ghosts' were similar in appearance to surface patterns observed by CSEM where root hairs had developed in the field while appressed against a hard surface (cf. Fig. 9C with Fig. 9A, B).

Mesh surfaces were colonized by only a few fungal hyphae (Fig. 9A, B). CSEM of root-hair surfaces showed some possible bacterial colonies (Fig. 9D), and, occasionally, apparent exudation from the tips of young root hairs (arrowheads Fig. 9E).

Change in phosphorus concentrations during root maturation

Total [P] decreased markedly from the youngest to the oldest segments (Fig. 10). The youngest had [P] > 1 mg g^{-1} d. wt. The next older segments coincided with the beginning of cortical maturation, and had, not surprisingly, 14-fold less [P] than the first segments which included the meristematic and elongating cells. Therefore, we used [P] of the second segments as a base value of 100 % for comparing total root [P] change as the cortex and epidermis matured. By segment 4, which included the region where the epidermis and cortex were dead but residual (Fig. 5), [P] was 0·017 mg g^{-1} d. wt, a decrease of 76 % during maturation of the cortex and epidermis.

DISCUSSION

Prologue

More than a century ago, Massart (1898, quoted in Price, 1911) elegantly described sandbinding roots of desert plants: 'wie das Bein in der Hose, oder besser und ästhetischer ausgedrückt, wie eine Phryganeenlarve in dem selbst gebauten Gehäuse' [like the leg in a pair of trousers, or put better and more aesthetically appealing, like a *Phryganea* larva (caddisworm) in its self-made case]. Although these larval cases, which comprise sand grains held together by silken threads spun out by the insect, resemble morphologically the root-enclosing sandsheaths, we find that a much more integrated development of root structure and sand grain recruitment is involved in sandsheath formation and persistence.

Our study has, for the first time, followed sandsheath development in detail and shows clearly that the sheath per se is only one component of a structural (certainly also multifunctional) unit that includes persistent root hairs, epidermis, inner and outer sclerified rims of cortex, and a lysigenous central cortex. We consider that this root/sandsheath structural unit contributes to survival of the perennial roots of *Lyginia* in the harsh sandplain environment, not only while these outer plant tissues involved are alive, but for long after they have died.

The root developmental pattern associated with the sandsheaths of the rush does resemble that of other desert and dune-adapted monocotyledonous species for which micrographs of the sheath and cortical anatomy have been recorded (e.g. Wullstein and Pratt, 1981, figs 2–4; Bergmann *et al.*, 2009, fig. 1), and most clearly, fig. 1 of Buckley (1982). But our findings also bring into focus similar root developmental features that have been noted occasionally in the literature (particularly very old literature), but are not generally in the mainstream information available on root structural properties of herbaceous monocotyledons. This information is included to stimulate interest in its relevance to root function, not

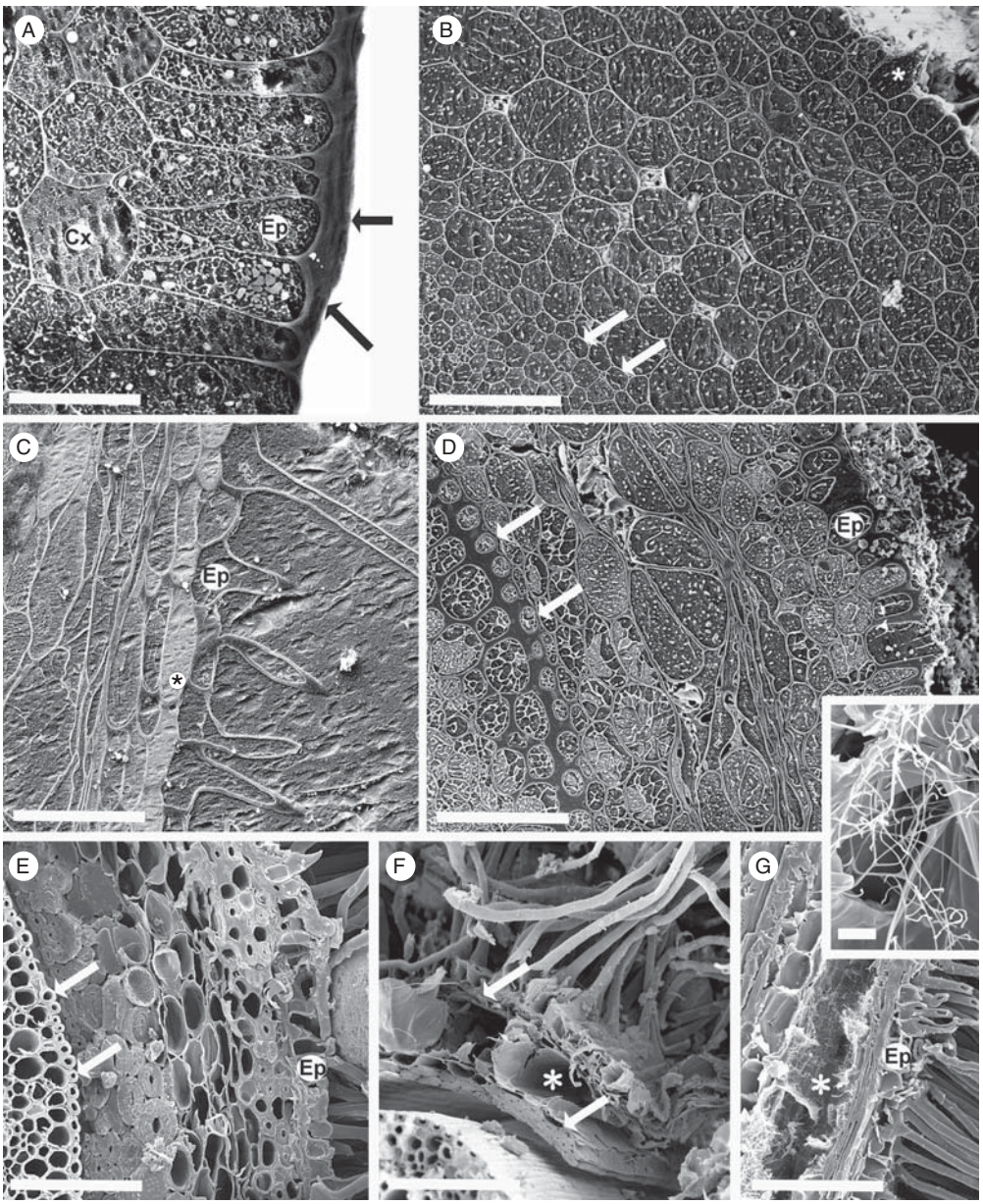

FIG. 5. (A–D) Roots frozen in the field, cryo-planed; CSEM. (E–G) Hand-cut, frozen in the cryo-microscope. (A) 2 mm from the root tip, root hairs not yet emerged. A thick pellicle (arrows) forms the epidermal (Ep) surface, cortex (Cx) intact and thin-walled. (B) Approx. 10 mm from the tip, root hairs emerging (asterisk). The epidermal pellicle had thinned and walls of epidermis, cortex and endodermis (arrow) were thin. (C) Approx. 50 mm from the tip, a hair has developed from each epidermal cell (Ep). Vacuoles of the subepidermal layer have possible phenolic contents (asterisk). (D) Approx. 75 mm from the tip. Root hairs removed. Walls (inner tangential and radial) of endodermis (arrows) and walls (outer tangential and radial) of epidermis (Ep) had thickened. Mid-cortical cells collapsing and air spaces evident. (E) Approx. 135 mm from the tip, the cortex comprising outer and inner rims of fibres; and senescing central region. Ep, epidermis; arrows, endodermis. (F, G) Older regions, central cortex aerenchymous (asterisks), enclosed by persistent epidermis and inner and outer layers of fibres (arrows). (G) Actinobacteria in the aerenchyma (asterisk), detail in inset. Thick walls of root hairs were evident where fractured. Ep, epidermis. (C) and (G) show longitudinal faces; others are transverse. Scale bars: (A) = 35 μm; (B) = 100 μm; (C) = 80 μm; (D) = 125 μm; (E) = 150 μm; (F) = 175 μm; (G) = 150 μm; inset = 8 μm.

only in extreme arid regions but also in native and cultivated mesophytic environments.

Development of the root/sandsheath structural unit in relation to sheath coherence and persistence

Root hairs. The key role of the root hairs in the development of the *Lyginia* sandsheaths was established definitively by field experiments (Figs 7 and 8). Sand grains were entrapped by hairs with no evidence of their coherence by mucilage (Fig. 8C), unlike the strong cohesion of soil particles by maize root-cap mucilage (Watt *et al.*, 1993). Where no hairs penetrated rigid fine mesh separating them from adjacent sand grains, no sheath formed on the underside of the mesh. With coarser meshes, the extent of sheath formation on the underside depended on the degree of hair penetration.

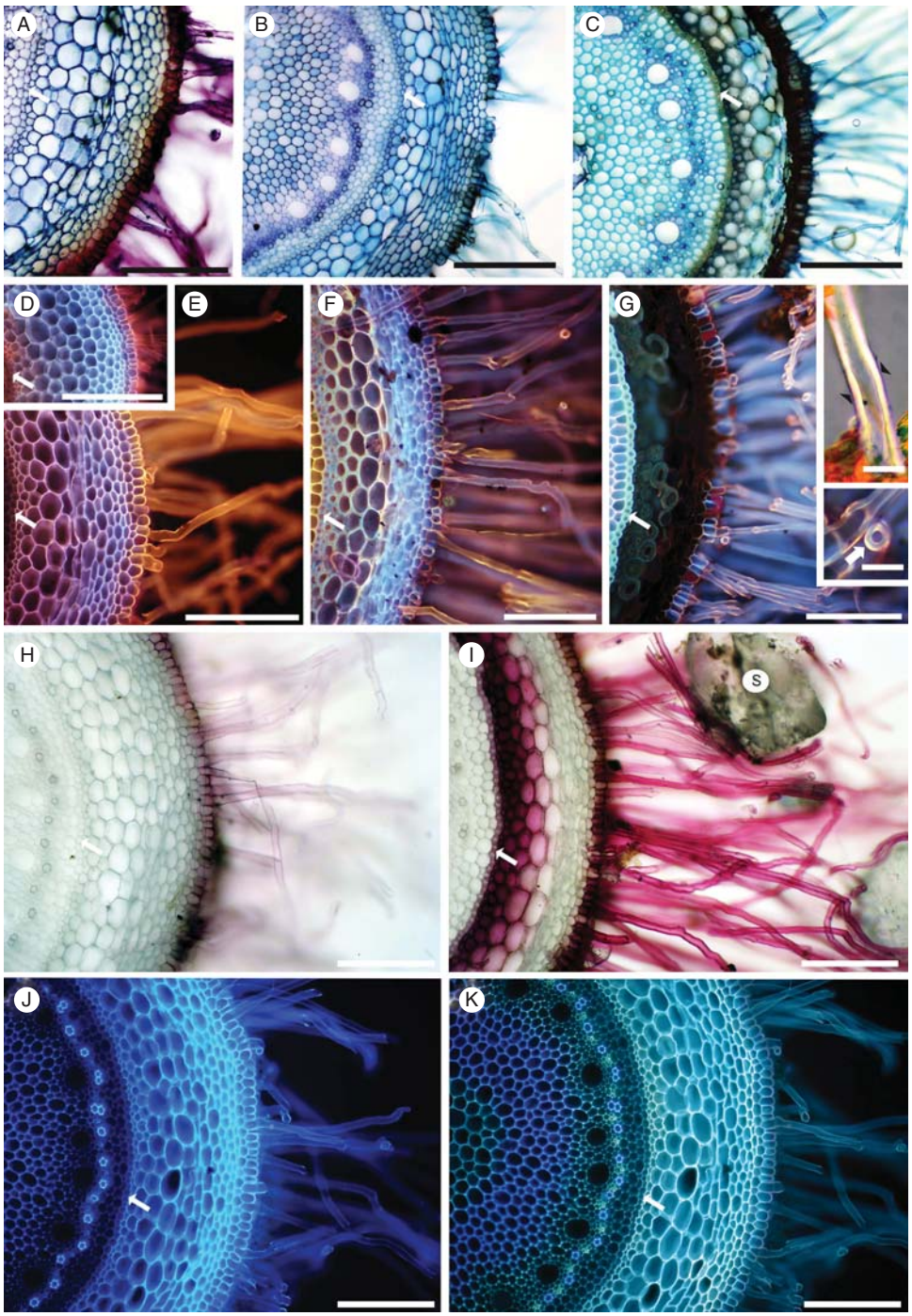

FIG. 6. Fresh, hand-cut transverse sections of roots after removal of sand grains. The endodermis (arrow) is toward the left of each micrograph. Approximate distance (mm) of each section from the root tip is indicated. (A–C) Toluidine blue stain, at 10, 20, and 100 mm, respectively. (D–G) Rhodamine B-induced fluorescence at 10, 20, 100 and 180 mm, respectively. (Insets, G) Root hairs at 180 mm. A thin Sudan-positive layer (arrowheads) overlies thick, birefringent walls (upper inset G). Magnification of transverse view (arrow) of root hair (lower inset G). (H, I) Phloroglucinol/HCl (Wiesner test) at 20 and 100 mm, respectively. S, sand grain. (J, K) UV-induced autofluorescence of the same section at 20 mm, (J) in water and (K) in 0·1 M ammonium hydroxide. Scale bars: (A) = 200 μm; (B) = 300 μm; (C) = 250 μm; (D) = 275 μm; (E) = 175 μm; (F) = 200 μm; (G) = 150 μm; insets = 20 μm; (H) = 150 μm; (I) = 225 μm; (J, K) = 150 μm.

The very high density of root hairs, their particular wall properties and persistence, and their tight adherence to sand grains are major factors in the formation and persistence of the perennial sandsheaths. Hair density (Table 2a) is far higher than published values for mesophytic grasses (Table 2b), but is very similar to the value for the Proteaceous species *Leucadendron laureolum* (800 root hairs mm^{-2} for proteoid rootlets, 530 for other roots) also native

TABLE 3. *Wall staining properties of root hairs and cells of outer, middle and inner cortex in fresh sections of roots of* L. barbata. *Observations were made from each of 10–20 roots.*

Distance from tip (mm)	Stain*	Root hair (rh), epidermis (ep)	Outer cortex	Middle cortex	Inner cortex	Figure
~10	TB	Pink/red	Blue	Blue	Blue	Fig. 6A
	RdB†	Light orange	–	–	–	Fig. 6D
	PG	rh base faint, ep +	–	–	–	Fig. 6H
~20	TB	Blue/green	Blue/green	Blue/green	Blue/green	Fig. 6B
	RdB	rh and ep bright orange	–	–	–	Fig. 6E
	PG	rh base faint, ep +	Ni	Ni	Ni	Ni
~100	TB	rh blue, ep blue/brown	Brown/blue	Greenish	Dark blue	Fig. 6C
	NS		Dark brown			Ni
	RdB	Orange/blue	–	–	–	Fig. 6F
	PG	+++	faint	–	+++	Fig. 6I
~180	TB	Dark green	Dark brown	Brown	Dark green	Ni
	NS	Grey/brown	Brown	Light brown	Brown	Ni
	RdB	rh, orange outer layer	–	–	–	Fig. 6G
	PG	+++	+++	–	+++	Ni

Ni = not illustrated.

* TB, Toluidine blue; RdB, Rhodamine B-induced fluorescence; PG, Phloroglucinol/HCl; NS, not stained, brown endogenous pigment. + = Positive reaction; intensity of staining (+) clear positive staining to (+++) intense positive staining. − = no staining reaction/colours.

† Rhodamine B outer, middle, inner cortex (–). We record only the yellow to bright orange fluorescence induced by this fluorochrome, which is known to indicate lipidic material (see text). Other colours in the sections result from underlying autofluorescence, non-fluorescent staining and endogenous pigment which may or may not have masked a positive reaction.

FIG. 7. The arrangement to test whether sandsheaths were formed by roots separated from soil by mesh of different pore size (see text). Scale bar = 100 mm.

to the Western Australian sandplains (Lamont, 1983). We found no density counts for other desert and sand dune perennial monocotyledons, but images such as those of Wullstein and Pratt (1981) suggest these plants have similarly high numbers.

Root-hair density counts available for mesophytic grasses are mainly from seedlings grown in the laboratory or young plants grown in pots where moisture levels were uniformly relatively high, although it is well established that root hair production by such species is stimulated by low soil moisture (e.g. Mackay and Barber, 1987). Indeed, root hairs on sonicated, field-grown sheathed roots of *Triticum aestivum* (Goodchild and Myers, 1987, fig. 3) are much more numerous than the number given for this species in Table 2(b), suggesting that the very high counts for the sandplain natives are not unique to these species.

The thick walls of mature *Lyginia* root hairs (Fig. 3C, D) are in marked contrast to the thin, fragile walls of 'normal' hairs described for most species (almost entirely from young laboratory-grown plants) in the modern literature. It is not possible to determine with certainty from the published images of grass sandsheaths (e.g. figures in Wullstein and Pratt, 1981) if the hair walls are thickened, but they appear collapsed, unlike the firm cylindrical shape of the *Lyginia* hairs, suggesting a weaker wall structure (or possibly a result of harsh preparative treatment). Thick-walled root hairs of *Lyginia* are not, however, unique. Von Guttenberg (1968) reports hairs with strongly thickened walls in the Restionaceae, and illustrates one of *Restio bifidus* with a wall approx. 3 μm thick. Von Guttenberg (1968) also reports that Hesse (thesis, 1902) frequently found thick-walled hairs in species growing in dry environments. Root hairs with walls 2 μm and up to 3 μm thick occur in *Gleditsia* and Gymnosperms, respectively (McDougall, 1921; Dittmer, 1948). Hair wall thickness in field-grown mesophytic herbaceous plants is unknown.

Our histochemical results show progressive changes in wall components of *Lyginia* root hairs, which reveal a complex chemistry beyond the cellulose and acidic polysaccharide (with some protein) wall components generally reported for 'normal' root hairs. Acidic polysaccharide is prominent in

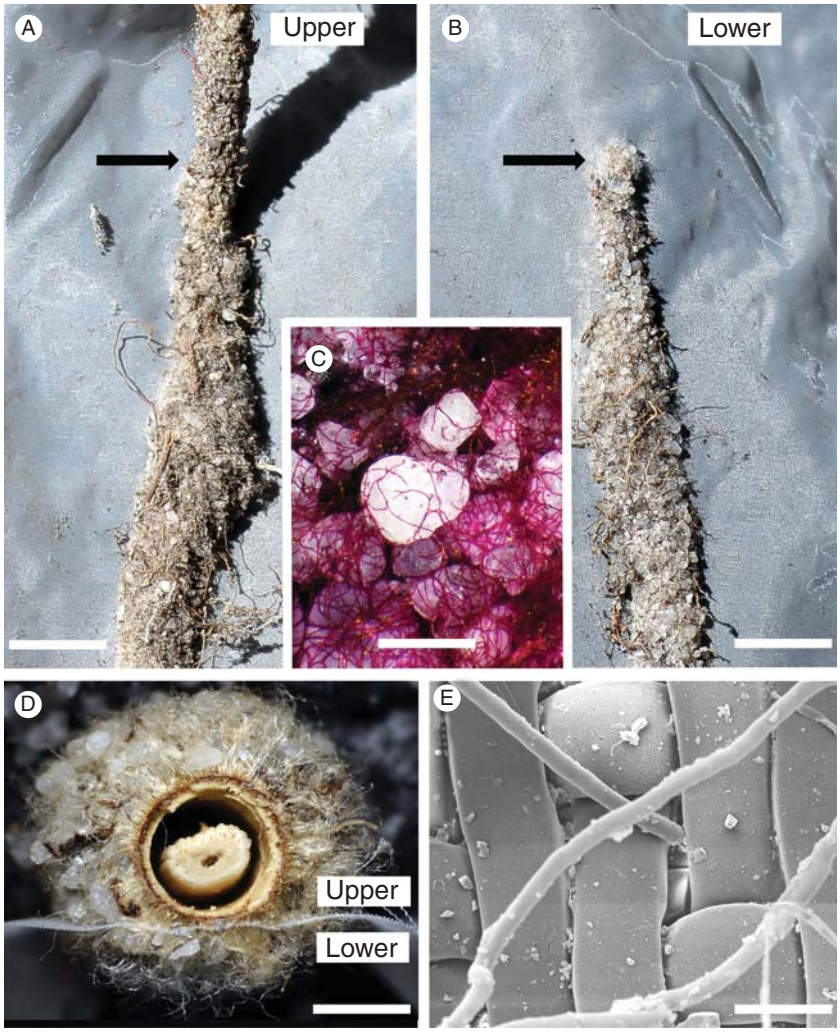

FIG. 8. Sandsheath formation by roots growing in contact with mesh screens in the field (Fig. 7). (A) Sheath on the upper side of a root growing downward over a nylon screen (38-μm pores) beyond where the root tip first contacted the mesh (arrow) the sheath was firmly attached to both root and mesh and was somewhat wider than in the unattached portion. (B) Underside of the same piece of mesh. A broad sheath was firmly attached to the mesh beyond the point (arrow) where the root tip first contacted the upper side of the mesh. Some senescent fine roots of unknown origin and other debris were incorporated into the sheaths. (C) Detail of sand grains and tangled root hairs on the underside of the mesh (PAS reaction). (D) Transverse section of root with sheath development on each side of nylon mesh (1-μm pores). Note the coherence of the residual epidermis/cortex complex to the sheath, and the shrunken stele, due to dehydration. (E) Small sheaths formed on the underside of mesh of 1-μm mesh, as root hairs were able to displace the fibres slightly and squeeze through to the lower side. CSEM. Scale bars: (A, B) = 7 mm; (C) = 680 μm; (D) = 1·25 mm; (E) = 52 μm.

walls of the youngest hairs and epidermis (Fig. 6A) but its pink metachromasy is masked by the early incorporation of compounds that stain blue/green with Toluidine blue and are autofluorescent blue/green to blue. These compounds include ferulic acid (Fig. 6B, C, J, K), and in older hairs, lignin (Fig. 6H, I). Beyond 20 mm from the root tip, the lipid-rich, yellow/orange fluorescent component (revealed by Rhodamine B), which initially appears in epidermal and young hair walls, is progressively masked by the blue/green autofluorescence (Fig. 6D–G) but remains as a clearly defined outer layer on mature hairs (Fig. 6G and lower inset). This lipid-rich layer coincides with the Sudan-positive layer outside the thick birefringent (cellulose-rich), lignified wall (Fig. 6G, upper inset). This layer is probably suberin, but a definitive identification awaits the application of acid digestion, and chemical analysis.

The composition of the walls of the *Lyginia* root hairs as revealed by histochemistry is unusual, but is not unique. A thin, lipid-rich surface layer (identified as suberin or cuticle) was shown for root hairs of a variety of cultivated species (Scott, 1950; Scott *et al.*, 1958; Dawes and Bowler, 1959) by lipid staining, and the persistence of the layer after H_2SO_4 digestion. A root epidermal wall component, also identified as suberin by histochemical stains and resistance to H_2SO_4 digestion, has been reported for a variety of species (Wilson and Peterson, 1983; Thomas *et al.*, 2007), and in the latter study the presence of suberin was confirmed chemically, Curiously, however, neither report mentions root hairs, but close examination of Thomas *et al.* (2007, fig. 1E) reveals that root hairs of soybean appear resistant to H_2SO_4 digestion. The implications of the lipid-rich coating for wall permeability and root hair function have not been investigated,

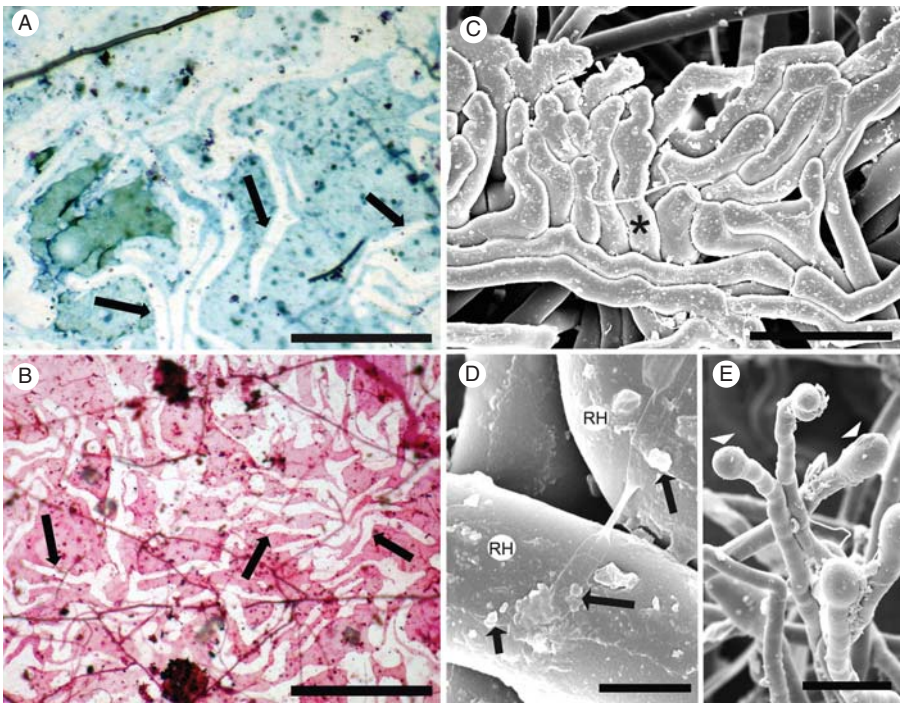

FIG. 9. (A, B) Upper surface of mesh (0·03-μm pores) after 3 months in the field, along which a root grew, but no root hairs penetrated, and no sandsheath formed on the underside. After the root was removed gently, unstained root hair 'ghosts' (arrows) were revealed by 'negative staining' with Toluidine blue (A) and Schiff's reagent (B). Mesh between the 'ghosts' stained lightly by both methods. Fungal hyphae (arrowheads). (C) Root hairs, constrained by a hard surface (e.g. asterisk, Fig. 2B) form tissue-like closely adhering pads resembling the 'ghost hair' images in A and B. (D) Sparse deposits of possible mucilage and microbial colonies (arrows) on old hair surfaces (RH). (E) Possible exudates from young hairs. (C–E) CSEM. Scale bars: (A) = 140 μm; (B) = 140 μm; (C) = 75 μm; (D) = 6 μm; (E) = 80 μm.

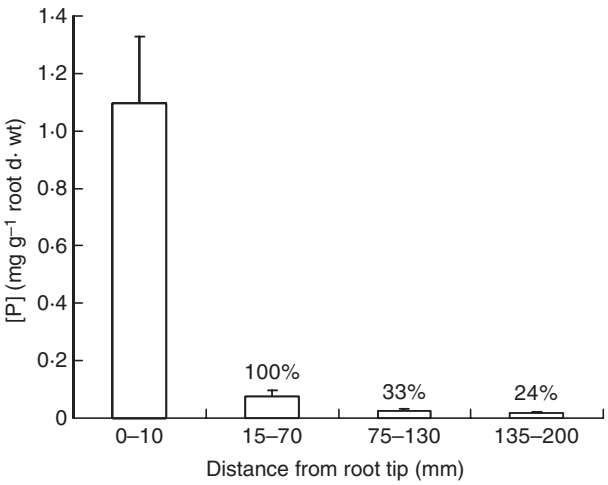

FIG. 10. Phosphorus concentrations in four regions along roots, from growing tips to a region of complete epidermal and cortical senescence. To better relate change in whole root [P] as this senescence progresses [P] was expressed as a percentage of that in the first region where root elongation is complete, which is set arbitrarily at 100 % (± s.e., $n = 7$).

although suberized root hairs are widely reported in the early literature (Von Guttenberg, 1968).

All the thick root hair walls mentioned by Von Guttenberg (1968) were also reported to be lignified, except those of *Gleditsia* (McDougall, 1921), but the brown, endogenous wall pigment of those hairs probably masked the aldehyde groups necessary for a positive phloroglucinol reaction (Pomar *et al.*, 2002), as also with the old sclerified epidermis and cortex (see below).

The longevity of the *Lyginia* sandsheaths requires persistence of the enmeshing root hairs, and persistent root hairs are described in all accounts of sandsheaths on perennial grasses (e.g. Price, 1911: Wullstein and Pratt, 1981; Buckley, 1982). In *Lyginia* this persistence of the walls of long-dead hairs is clearly the result not only of their thick, cellulose walls, but also the early incorporation of recalcitrant compounds such as ferulic acid, lignin and probably suberin.

In general it is assumed that normal root hairs are short-lived, functioning for only a few days, then collapsing and dying (e.g. Jungk, 2001). But this assumption is almost always based on observations of unstressed plants. It is, however, reported occasionally that the walls of root hairs of herbaceous plants, particularly grasses, growing under field or stressed conditions, can persist for the life of the plants (e.g. Weaver, 1925; Henrici, 1929; Goossens, 1936; Dittmer, 1946, 1949), and even that they may remain functional for about 7 weeks in wheat (Weaver, 1925), although the latter claim needs confirmation. The chemistry of the hair walls which supports this persistence is still unclear, but there is evidence that recalcitrant compounds are also present, as in the *Lyginia* hairs.

Clarkson *et al.* (1987) found that the walls of root hairs that persisted at the base of maize adventitious roots were totally

resistant to strong wall-hydrolysing enzymes. Mort and Grover (1988) reported that only approx. 80 % of the root hair walls of grasses was carbohydrate, with a small protein fraction. Knirel *et al.* (1989) added that these walls and those of the epidermis included a polyphenol component, and they quoted Hamilton and Mort (unpublished) that 'the presence of visibly intact root hair walls after hydrogen fluoride solvolysis and trypsin treatment . . . (indicates) . . . a substantial amount of lignin-like material in root hair (walls)'. The functional significance of persistent root hair walls of field-grown mesophytic grasses remains to be revealed.

Epidermis and sclerified outer cortical rims. Unlike the disintegrating epidermis of many monocotyledonous roots, the thick-walled, dead epidermis persists in mature *Lyginia* roots. The strongly lignified walls are tightly adherent to each other, to their lignified root hairs and the heavily sclerified subtending outer cortical rim (Fig. 6F–I). In older regions the dead epidermis/outer cortical rim is infiltrated by deep brown pigment (Figs 4A and 8D), possibly oxidized phenols or quinoidal compounds as described in old endodermal walls (Van Fleet, 1961). This pigment inhibits staining and autofluorescence of these layers, and must enhance the persistence of this stable platform, which holds the hairs in place, thus indirectly maintaining the tight coherence and shape of the perennial sheaths (Figs 4A and 8D). The strongly lignified inner rim of cortical fibres (Fig. 5E, F), which also becomes brown with age (Figs 6C, G, I; Shane *et al.*, 2010, fig. 7d) adds stability to the structural unit and maintains the space of the lysigenous mid-cortex component.

What functional roles are played by the structural unit?

To date there is no definitive evidence for roles played by the sandsheath/root structural unit of *Lyginia*, and these must remain speculative until experimental evidence is obtained. A range of possible functions has been suggested in the literature for similar structural features of roots in arid environments, only occasionally based on experimental data. The following is a discussion of some of these possibilities.

Accumulation and retention of sparsely available water and nutrients. (*a*) Water and nutrient acquisition. The close tracking of *Lyginia* root hairs around sand grains (Fig. 3) suggests a thigmotropic response. However, in the only detailed study of root hair irritability, Seidel (1924) found no evidence for thigmotropism, and his clear demonstration of hairs bending into and tightly around soil particles and tiny samples of specific nutrients suggested chemotropism. Hairs of different species were differentially attracted by specific nutrients, including phosphate and nitrate. This phenomenon could well apply to *Lyginia* root hairs, as scarce nutrients are probably enriched in the cutan coatings of the sand grains (Jensen *et al.*, 2002) where they and thin films of water would be accessed by the closely adherent living root hairs in the distal regions of the roots.

(*b*) Prevention of water loss from mature regions. Beginning with the earliest description of sandsheaths of perennial roots of desert grasses (Volkens 1887, as quoted by Fahn and Cutler, 1992), authors have speculated that these sheaths prevent water loss from the still functioning parts of the perennial roots, Volkens suggesting they replace the corky periderms of dicotyledon roots. The desert and dune grasses in which sandsheaths have been described are, like *Lyginia*, perennials. Indeed, Danin (1996) in a study of numerous species of the grass genus *Stipagrostis* in sand dunes in Israel found that only the perennials formed sandsheaths, whereas annuals and annual forms of perennial species did not.

Those perennial roots of *Lyginia* and other drought-resistant monocotyledons (e.g. the Mediterranean grass *Phalaris tuberosa*, McWilliam and Kramer, 1968), which access deep moisture during the dry season, are the only source of water for the culms, and indirectly, the younger short roots that remain dormant in the bone-dry upper part of the sand profile. Prevention of water loss from their steles to the dry soil is critical, not only for maintenance of transport function in both xylem and phloem, but also for maintenance of pericycle and stelar tissues involved in the development of fine feeder roots in the wet season. One or more components of the non-living structural unit enclosing the stele of mature *Lyginia* roots occur in all perennial roots of monocotyledons that have been described from dry environments, with frequent speculation that each is involved in water retention. The most experimental work supporting such claims has been with a non-sheath-forming desert succulent, *Agave deserti*, by Nobel, North and co-workers (e.g. North and Nobel, 1995), who have shown large reductions in radial hydraulic conductance by sclerified inner and outer cortical rims, and particularly also by a lysiginous cortex. The impermeability of a heavily sclerified outer cortex in another monocotyledon, *Carex arenaria*, was definitively demonstrated by Robards *et al.*, 1979). The best evidence for protection from water loss by root sheaths is, however, from two dicotyledon desert species, *Ferrocactus acanthodes* and *Opuntia ficus-indica*, in which sheathed roots exposed to dry air had over 50 % lower radial hydraulic conductance than similar roots from which the sheaths had been removed (North and Nobel, 1992). No direct data are available for the permeability of sandsheaths of monocotyledons, but Wullstein *et al.* (1979) found that the water content of sandsheaths of four xeric grasses varied, on a dry weight basis, from 12 to 25 % while surrounding sand varied from 3 to 8 %, suggesting some protection against water loss. Thus, all components of the non-living structural unit that surrounds the living steles of the perennial *Lyginia* roots are together probably providing an effective barrier to water loss.

(*c*) Recycling of scarce nutrients. The results of P analysis along the *Lyginia* roots (Fig. 10) suggest that the young cortex accumulates P while its cells are alive, but this P disappears as the cortex senesces. Some or most of this 'lost' P may have been recovered by the adjacent living tissues of the stele. Remobilization of accumulated P has been hypothesized as a major function of cortical senescence in cereal roots (Robinson, 1990), and would be particularly advantageous for perennial roots in the nutrient-poor environment of the sandplains. The possibility of such conservation of P and other nutrients in *Lyginia* warrants further investigation.

Provision of a protective environment for beneficial microbes. There are suggestions that some desert and dune grasses that

form perennial sandsheaths may be benefiting from N_2-fixing bacteria associated with the sheath and underlying senescent tissue. This possibility is based on findings of acetylene reduction associated with sandsheaths, and/or diazotrophic bacteria isolated from the sheaths (Wullstein *et al.*, 1979; Wullstein, 1991; Othman *et al.*, 2004; Bergmann *et al.*, 2009). Wullstein *et al.* (1979) speculated that increased water retention and low O_2 tension within the compact sheath provide conditions necessary for N_2 fixation. The possibility of N_2 fixation and utilization by *Lyginia* and other sandsheath-formers of the sandplains remains to be investigated.

Our observation of actinobacteria as the common microbes within the dead cortex suggests that these organisms, well known for their antimicrobial properties, may play an essential role in protecting the long-lived functioning steles. The persistent cortex/sheath complex, by providing a preferred environment for these organisms, could form (as termed by Sivasithamparam, 1998) the 'final frontier' against invading pathogens. We note the rare occurrence of fungi in the sheaths and dead tissues.

Provision of mechanical strength and protection of the perennial roots. Sandsheath encasement would certainly appear to protect the long-lived roots from herbivory, although again there are no observational data to support this. However, one occasionally finds evidence of their resistance to invasion by the aggressive hemiparasite *Nuytsia floribunda*, ubiquitous in their environment (Fig. 4B). Such haustorial encirclement is relatively unusual, and sections through the encircled regions show no invasion through the sheath.

Providing long-lasting channels in the sand profile. Price (1911) and Arber (1934) noted that sandsheaths retained their shape when dry, even on a herbarium sheet. Figure 8D demonstrates that in dried pieces of *Lyginia* roots, the sheath with the rest of the functional unit also retains its shape, while the stele shrinks. In dead roots, the central space may persist as a vertical channel in the sand profile, maintained by the rigid sheath complex. Thus, relict sandsheaths could form preferential flow paths for water and air to reach deep into the profile, and/or act as channels to facilitate rapid decent of young roots of *Lyginia* or other local species.

ACKNOWLEDGEMENTS

This work was supported by grants DP1092856 and DP0663243 from the Australian Research Council (ARC) to M.W.S., an ARC Australian Research Fellow.

LITERATURE CITED

Arber A. 1934. *The Gramineae: a study of cereal, bamboo, and grass.* Cambridge: Cambridge University Press.

Bergmann D, Zehfus M, Zierer L, Smith B, Gabel M. 2009. Grass rhizosheaths: associated bacterial communities and potential for nitrogen fixation. *Western North American Naturalist* **69**: 105–114.

Bailey C, Scholes M. 1997. Rhizosheath occurrence in South African grasses. *South African Journal of Botany* **63**: 484–490.

Boerner D. 1952. Fluorezenzmikroskopische Untersuchungen an Lipoiden. *Protoplasma* **41**: 168–177.

Boot RGA, Mensink M. 1990. Size and morphology of root systems of perennial grasses from contrasting habitats as affected by nitrogen supply. *Plant and Soil* **129**: 291–299.

Buckley R. 1982. Sand rhizosheath of an arid zone grass. *Plant and Soil* **66**: 417–421.

Clarkson DT, Robards AW, Stephens JE, Stark M. 1987. Suberin lamellae in the hypodermis of maize (*Zea mays*) roots: development and factors affecting the permeability of hypodermal layers. *Plant, Cell and Environment* **10**: 83–94.

Craig S, Beaton CD. 1996. A simple cryo-SEM method for delicate plant tissues. *Journal of Microscopy* **182**: 102–105.

Danin A. 1996. Adaptations of *Stipagrostis* species to desert dunes. *Journal of Arid Environments* **34**: 297–311.

Dawes CJ, Bowler E. 1959. Light and electron microscope studies of the cell wall structure of the root hairs of *Raphanus sativus*. *American Journal of Botany* **46**: 561–565.

Dittmer HJ. 1946. A critical study of subterranean plant parts. *American Journal of Botany* **33**: 819.

Dittmer HJ. 1948. Root hair development on Gymnosperm seedlings. *American Journal of Botany* **35**: 791.

Dittmer HJ. 1949. Root hair variations in plant species. *American Journal of Botany* **36**: 152–155.

Dittmer HJ. 1958. A quantitative study of the subterranean members of three field grasses. *American Journal of Botany* **25**: 654–657.

Dodd J, Heddle EM, Pate JS, Dixon KW. 1984. Rooting patterns of sandplain plants and their functional significance. In: Pate JS, Beard JS. eds. *Kwongan – plant life of the sandplain*. Nedlands, Australia: University of Western Australia Press, 146–177.

Drew MC, Nye PH. 1969. The supply of nutrient ions by diffusion to plant roots in soil. II. The effect of root hairs on the uptake of potassium by roots of rye grass (*Lolium multiflorum*). *Plant and Soil* **31**: 407–424.

Evans H. 1938. Studies on the absorbing surface of sugar-cane root systems. 1. Method of study with some preliminary results. *Annals of Botany* **11**: 159–182.

Fahn A, Cutler DF. 1992. *Xerophytes. Encyclopedia of plant anatomy*. Berlin: Gebrüder Borntrager.

Föhse D, Claassen N, Jungk A. 1991. Phosphorus efficiency of plants II. Significance of root radius, root hairs and cation–anion balance for phosphorus influx in seven plant species. *Plant and Soil* **132**: 261–272.

Goodchild DJ, Meyers LF. 1987. Rhizsheaths- a neglected phenomenon in Australian agriculture. *Australian Journal of Agricultural Research* **38**: 559–563.

Goossens AP. 1936. Notes on the anatomy of grass roots. *Transactions of the Royal Society of South Africa* **23**: 1–21.

Harris PJ, Hartley RD. 1976. Detection of bound ferulic acid in cell walls of the Gramineae by ultraviolet fluorescence microscopy. *Nature* **259**: 508–510.

Henrici M. 1929. The cortex of grass roots in the more arid regions of South Africa. *Union of South Africa Department of Agriculture Science Bulletin* **85**: 3–12.

Hill JO, Simpson RJ, Ryan MH, Chapman DF. 2010. Root hair morphology and mycorrhizal colonization of pasture species in response to phosphorus and nitrogen nutrition. *Crop and Pasture Science* **61**: 122–131.

Huang CX, Canny MJ, Oates K, McCully ME. 1994. Planing frozen hydrated plant specimens for SEM observations and EDX microanalysis. *Journal of Microscopy Research and Technique* **28**: 67–74.

Jensen MB, Hansen HCB, Magid J. 2002. Phosphate sorption to macropore wall materials and bulk soil. *Water, Air and Soil Pollution* **137**: 41–48.

Jensen WA. 1962. *Botanical histochemistry*. San Francisco, Freeman.

Jungk A. 2001. Root hairs and the acquisition of plant nutrients from soil. *Journal of Plant Nutrition and Soil Science* **164**: 121–129.

Knirel YA, Vinogradov EV, Mort AJ. 1989. Application of anhydrous hydrogen fluoride for the structural analysis of polysaccharides. *Advances in Carbohydrate Chemistry and Biochemistry* **47**: 167–202.

Lamont B. 1983. Root hair dimensions and surface/volume/weight ratios of roots with the aid of scanning electron microscopy. *Plant and Soil* **74**: 149–152.

Mackay AD, Barber SA. 1987. Effect of cyclic wetting and drying of a soil on root hair growth of maize roots. *Plant and Soil* **104**: 291–293.

McArthur WM. 1991. *Reference soils of south-western Australia*. Perth, Australia: Department of Agriculture.

McCully ME. 1999. Roots in soil: unearthing the complexities of roots and their rhizospheres. *Annual Review of Plant Physiology and Plant Molecular Biology* **50**: 695–718.

McCully ME, Canny MJ. 1994. Contributions of the surface of the root tip to the growth of *Zea* roots in soil. *Plant and Soil* **165**: 315–321.

McCully ME, Shane MW, Baker AN, Huang CX, Ling LEC, Canny MJ. 2000. The reliability of cryoSEM for the observation and quantitation of xylem embolisms and quantitative analysis of xylem sap *in situ*. *Journal of Microscopy* **198**: 24–33.

McCully ME, Canny MJ, Huang CX, Miller C, Brink F. 2010. Cryo-scanning electron microscopy (CSEM) in the advancement of functional plant biology: energy dispersive X-ray microanalysis (CEDX) applications. *Functional Plant Biology* **37**: 1011–1040.

McDougall WB. 1921. Thick-walled root hairs of *Gleditsia* and related genera. *American Journal of Botany* **8**: 171–175.

McWilliam JR, Kramer PJ. 1968. The nature of the perennial response in Mediterranean grasses. 1. Water relations and summer survival *in Phalaris*. *Australian Journal of Agricultural Research* **19**: 381–395.

Meney KA, Pate JS. 1999. *Australian rushes – biology, identification and conservation of Restionaceae and allied families.* Nedlands, Australia: University of Western Australia Press.

Moreno-Espindola IP, Rivera-Becerril F, Ferrara-Guerrero MJ, León-Gonzalez F. 2007. Role of root-hairs in adhesion of sand particles. *Soil Biology and Biochemistry* **39**: 2520–2526.

Mort AJ, Grover PB Jr. 1988. Characterization of root hair cell walls as potential barriers to the infection of plants by rhizobia. *Plant Physiology* **86**: 638–641.

Motomizu S, Wakimoto T, Toei K. 1983. Spectrophotometric determination of phosphate in river waters with molybdate blue and malachite green. *Analyst* **108**: 361–367.

North GB, Nobel PS. 1992. Drought-induced changes in hydraulic conductivity and structure in roots of *Ferocactus acanthodes* and *Opuntia ficus-indica*. *New Phytologist* **120**: 9–19.

North GB, Nobel PS. 1995. Hydraulic conductivity of concentric root tissues of *Agave deserti* Engelm. under wet and drying conditions. *New Phytologist* **130**: 47–57.

O'Brien TP, McCully ME. 1981. *The study of plant structure. principles and selected methods*. Melbourne: Termarcarphi.

Othman AA, Amer WM, Fayez M, Hegazi NA. 2004. Rhizosheath of Sinai desert plants is a potential repository for associative diazotrophs. *Microbiological Research* **159**: 285–293.

Pearse AGE. 1968. *Histochemistry. theoretical and applied*, Vol. 1. London: J and A Churchill.

Pomar F, Merino F, Ros Barceló A. 2002. *O*–4-linked coniferyl and sinapyl aldehydes in lignifying cell walls are the main targets of the Wiesner (phloroglucinol-HCl) reaction. *Protoplasma* **220**: 17–28.

Price SR. 1911. The roots of some North African desert grasses. *New Phytologist* **10**: 328–340.

Reid JB. 1981. Observations on root hair production by lucerne, maize and perennial ryegrass in a sandy loam. *Plant and Soil* **62**: 319–322.

Robards AW, Clarkson DT, Sanderson J. 1979. Structure and permeability of the epidermal/hypodermal layers of the sand sedge (*Carex arenaria* L.). *Protoplasma* **101**: 331–347.

Robinson D. 1990. Phosphorus availability and cortical senescence in cereal roots. *Journal of Theoretical Biology* **145**: 257–265.

Robinson SP, Rorison IH. 1987. Root hairs and plant growth at low nitrogen availabilities. *New Phytologist* **107**: 681–693.

Schweiger PF, Robson AD, Barrow NJ. 1995. Root hair length determines beneficial effect of a *Glomus* species on shoot growth of some pasture species. *New Phytologist* **131**: 247–254.

Scott FM. 1950. Internal suberization of tissues. *Botanical Gazette* **3**: 378–394.

Scott FM, Hamner KC, Baker E, Bowler E. 1958. Microscope studies of the epidermis of *Allium cepa*. *American Journal of Botany* **45**: 449–461.

Seidel K. 1924. Untersuchungen über das Wachstrum und die Reizbarkeit der Wurzelhaare. *Jarbücher für wissenschaftliche Botanik* **63**: 501–552.

Shane MW, McCully ME, Canny MJ, *et al*. 2009. Summer dormancy and winter growth: root survival strategy in a perennial monocotyledon. *New Phytologist* **183**: 1085–1096.

Shane MW, McCully ME, Canny MJ, *et al*. 2010. Seasonal water relations of *Lyginia barbata* (Southern rush) in relation to root xylem development and summer dormancy of root apices. *New Phytologist* **185**: 1025–1037.

Sivasithamparam K. 1998. Root cortex – the final frontier for the biocontrol of root-rot with fungal antagonists: a case study on a sterile red fungus. *Annual Review of Phytopathology* **36**: 439–452.

Thomas R, Fang X, Ranathunge K, Anderson TR, Peterson CA, Bernards MA. 2007. Soybean root suberin: anatomical distribution, chemical composition, and relationship to partial resistance to *Phytophthora sojae*. *Plant Physiology* **144**: 299–311.

Van Fleet DS. 1961. Histochemistry and function of the endodermis. *The Botanical Review* **27**: 165–220.

Von Guttenberg H. 1968. *Der Primäre Bau der Angiospermenwurzel*. Berlin: Gebrüder Borntraeger.

Watt M, McCully ME, Jeffree CE. 1993. Plant and bacterial mucilage of the maize rhizosphere: comparison of their soil binding properties and histochemistry in a model system. *Plant and Soil* **151**: 151–165.

Watt M, McCully ME, Canny MJ. 1994. Formation and stabilization of rhizosheaths in *Zea mays* L. Effect of soil water content. *Plant Physiology* **106**: 179–186.

Weaver JE. 1925. Investigations on the root habits of plants. *American Journal of Botany* **12**: 502–509.

Wilson CA, Peterson CA. 1983. Chemical composition of the epidermal, hypodermal, endodermal and intervening cortical cell walls of various plant roots. *Annals of Botany* **51**: 759–769.

Wullstein LH. 1991. Variation in N_2 fixation (C_2H_2 reduction) associated with rhizosheaths of Indian ricegrass (*Stipa hymenoides*). *American Midland Naturalist* **126**: 76–81.

Wullstein LH, Pratt SA. 1981. Scanning electron microscopy of rhizosheaths of *Oryzopsis hymenoides*. *American Journal of Botany* **68**: 408–419.

Wullstein LH, Bruening ML, Bollen WB. 1979. Nitrogen fixation associated with sand grain root sheaths (rhizosheaths) of certain xeric grasses. *Physiologia Plantarum* **46**: 1–4.